PAPER

S_{11} Calibration of Cut-Off Circular Waveguide with Three Materials and Related Application to Dielectric Measurement for Liquids

Kouji SHIBATA[†a)], ***Member***

SUMMARY A method for the calibration of S_{11} at the front surface of a material for a coaxial-feed type cut-off circular waveguide with three reference materials inserted and no short termination condition was proposed as a preliminary step for dielectric measurement in liquids. The equations for jig calibration of S_{11} with these reference materials were first defined, and the electrostatic capacitance for the analytical model unique to the jig was quantified by substituting the reflection constant (calculated at frequencies of 0.50, 1.5 and 3.0 GHz using the mode-matching (MM) technique) into the equivalent circuit, assuming the sample liquid in the jig. The accuracy of S_{11} measured using the proposed method was then verified. S_{11} for the front surface of the sample material was also measured with various liquids in the jig after calibration, and the dielectric constants of the liquids were estimated as an inverse problem based on comparison of S_{11} calculated from an analytical model using EM analysis via the MM technique with the measured S_{11} values described above. The effectiveness of the proposed S_{11} calibration method was verified by comparison with dielectric constants estimated after S_{11} SOM (short, open and reference material) calibration and similar, with results showing favorable agreement with each method.

key words: *dielectric measurement, liquid, cut-off circular waveguide, S_{11}, calibration*

1. Introduction

To comply with safety standards prescribing limits on exposure to EM (electromagnetic) waves, evaluation of the specific absorption rates (SARs) of various radio systems has recently become necessary [1]. Against this background, M. A. Stuchly et al. (1980) overviewed dielectric measurement for various lossy media based on reflected and transmitted EM waves with a sample in the middle or at the tip of a transmission line [2]. In the above research, dielectric measurement based on reflection coefficients with a sample in a cut-off circular waveguide placed at the tip of a coaxial line was also examined, but no actual dielectric measurement example with this jig shape was included in the published paper [2]. O. Göttmann et al. (1996) proposed dielectric measurement based on the reflection coefficient with a sample in both the coaxial line and the cut-off circular waveguide, which is placed at the tip of the connector [3]. In this method, the jig must be mounted after S_{11} calibration at the coaxial tip with a general SOL (short, open and load) calibration kit. Accordingly, measured S_{11} values and estimated dielectric constant are greatly affected by small differences in the length of the center conductor. Against this background, Shibata (2010) previously outlined the effectiveness of a high-precision broadband dielectric measurement method for small amounts of certain liquids based on S_{11} using a cut-off circular waveguide [4]. In this work, application of the mode-matching (MM) technique enabled calculation of S_{11} for an analytical model more quickly than with other approaches. As part of efforts to develop this method, the potential for dielectric measurement in liquids in the low frequency band, estimation using a simple formula and methods for improving measurement accuracy have also been presented [5]–[10]. Meanwhile, the coaxial probe (flange) method is commonly adopted to determine complex permittivity in solid and liquid high-loss electrical materials [11]–[13]. However, the dielectric constant changes significantly in the coaxial method due to EM wave reflection from the vessel, which hinders determination of uncertainty. As the sample in the proposed method is inserted into the cut-off circular waveguide section, the confinement of EM waves to this waveguide supports high measurement accuracy by eliminating the need to consider wave reflection from the vessel when the coaxial probe is used, thereby facilitating determination of permittivity in small amounts of scarce liquids. However, this method produces an error effect on S_{11} and the dielectric constant caused by the difference between the actual dimensions of the jig and the analytical model.

In this study, a method for the calibration of S_{11} based on the insertion of three reference materials with no short termination condition using a VNA (vector network analyzer) was newly proposed as a preliminary step for dielectric measurement in liquids via the cut-off circular waveguide reflection method. A calibration equation for S_{11} based on three impedance standards was first defined from the error model of the measurement system, and a theoretical value for a reflection constant based on the insertion of the three reference materials was also defined for equivalent circuit analysis of the analytical model. Here, the electrostatic capacitance for the analytical model unique to the jig was quantified by substituting the reflection constant (calculated using EM analysis via the MM technique) into the equivalent circuit, assuming the sample liquid in the jig. The S_{11} value for the jig was then calibrated from the

Manuscript received May 13, 2020.
Manuscript revised July 9, 2020.
Manuscript publicized August 14, 2020.

[†]The author is with Hachinohe Institute of Technology, Hachinohe-shi, 031–8501 Japan.
a) E-mail: shibata@hi-tech.ac.jp

DOI: 10.1587/transele.2020ECP5025

reflection constant with three reference materials (pure water, methanol and air) inserted using a VNA over the frequency band of 0.50–3.0 GHz. The validity of the calibrated S_{11} values obtained with the proposed method was verified via comparison with the S_{11} value measured after SOM (short/open and reference material (pure water)) calibration conditions [14]. S_{11} at the front surface of the sample was measured with various liquids in the jig after calibration with three reference materials, and the dielectric constants of various liquids were estimated from the above S_{11} based on an inverse problem approach involving comparison with the S_{11} value calculated using EM analysis via the MM technique [4], [10]. The results were compared with the permittivity values estimated as an inverse problem after SOM calibration conditions [14] and similar, with results showing favorable agreement of values determined with each method.

2. Dielectric Measurement Method and Related S_{11} Calibration Theory

In this method, the dielectric constant is estimated from the S_{11} value measured with various liquids in the cut-off waveguide with a coaxial feed-type SMA connector (Fig. 1). Here, a novel S_{11} calibration method involving the use of three reference liquids and no short termination is proposed as a preliminary step for dielectric measurement. The estimation procedure is as follows:

1. The measurement jig (a coaxial-feed-type cut-off circular waveguide with an SMA connector) is attached to a measurement cable connected to a VNA.
2. S_{11} is calibrated at the front surface of the sample of the jig with the three reference material inserted.
3. S_{11} at the front of the sample material is measured with various liquids in the jig.
4. The dielectric constant is estimated as an inverse problem so that the calculated S_{11} value for the jig-related analytical model corresponds to the measured value for each frequency.

The proposed S_{11} calibration method with three reference materials is outlined here. Calibration for S_{11} with a short condition – as applied in the previous stage of dielectric measurement of materials based on reflection coefficient differences with different samples in the jig – has previously been proposed (e.g., Ref. [15]). This procedure is applied in commercial products such as dielectric measurement kits involving the use of coaxial probes from Keysight Technologies [16]. However, there is concern regarding the instability of electrical contact with the inner surface of the outer conductor of the coaxial line using this structure, and related uncertainty in measured values of S_{11} and complex permittivity.

In this study, a reference material is used instead of load termination as a calibrator. S_{11} is also not determined with the coaxial tip short-circuited, but is measured with a second reference material inserted. Based on the above, S_{11} values determined with the three reference liquids in the jig are used for S_{11} calibration with this method. Accordingly, the theoretical values of S_{11} at the front surface of the sample with the three termination conditions must also be calculated from equivalent circuit analysis. Meanwhile, actual S_{11} values with these materials inserted are measured using the VNA. The S_{11} value for the front surface of the sample with insertion of an unknown material is then calibrated via substitution of these values into the equation described later. The equation for calibration of the coaxial line S_{11} value with the proposed method and the three reference materials is derived as outlined below. Equation (1) is first satisfied for the reflected wave b_1 observed with the EM wave a_1 incident from the measuring instrument in the two-terminal pair circuit of Fig. 3, which corresponds to the analytical model of Figs. 1 and 2.

$$\begin{bmatrix} b_1 \\ b_2 \end{bmatrix} = \begin{bmatrix} \dot{S}_{11} & \dot{S}_{12} \\ \dot{S}_{21} & \dot{S}_{11} \end{bmatrix} \cdot \begin{bmatrix} a_1 \\ a_2 \end{bmatrix} \tag{1}$$

The reflection coefficients for Ref. (Ports) 1 and 2 in Fig. 3 are then defined as ρ_i and Γ_i in Eqs. (2) and (3), corresponding to the these termination conditions:

$$\dot{\rho}_i = \frac{b_1}{a_1} \quad (2), \quad \dot{\Gamma}_i = \frac{a_2}{b_2} \tag{3}$$

Here, three termination conditions and one unknown material are then defined with insertion into the jig depending on subscripts 1, 2 and 3 for Γ_i and ρ_i.

Accordingly, the reflection coefficient ρ_i for Ref. 1 (Port 1) is calculated using Eq. (4) with systematic error term settings of $E_{DF} = S_{11}$, $E_{SF} = S_{22}$, $E_{RF} = S_{12}$ and $S_{21} = 1$ in Eqs. (1)–(3).

$$\dot{\rho}_i = \dot{E}_{DF} + \frac{\dot{\Gamma}_i \cdot \dot{E}_{RF}}{1 - \dot{E}_{SF} \cdot \dot{\Gamma}_i} \tag{4}$$

The reflection coefficient Γ_i for Ref. 2 (Port 2) is thus calculated as per [15] based on the following equation with replacement of Γ_i in Eq. (4):

$$\dot{\Gamma}_i = \frac{a_2}{b_2} = \frac{\dot{\rho}_i - \dot{E}_{DF}}{\dot{E}_{SF} \cdot \dot{\rho}_i + \dot{E}_{RF} - \dot{E}_{SF} \cdot \dot{E}_{DF}} \tag{5}$$

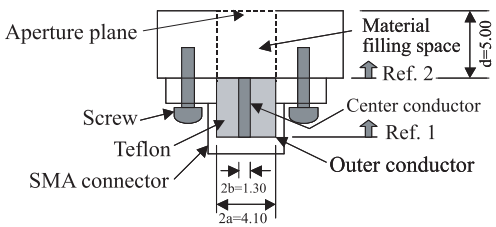

Fig. 1 Jig cross-section

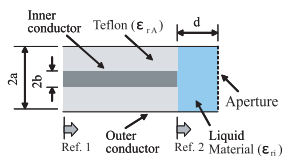

Fig. 2 Analytical model

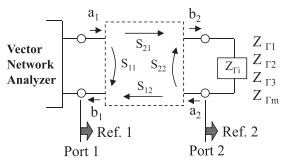

Fig. 3 Equivalent circuit

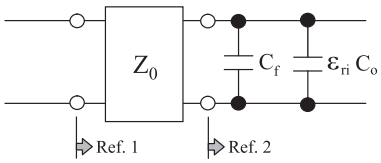

Fig. 4 Equivalent circuit

Here, Γ_i in Eq. (5) can be determined from the three unknowns of E_{DF}, E_{SF}, E_{RF} and γ by placing the denominator of Eq. (5) as γ and adapting the equation based on comparison of the association among Eqs. (1)–(3) and (4), (5) as in the following equation:

$$\dot{E}_{SF} = \frac{\dot{\rho}_2 - \dot{\rho}_3 + \dot{\gamma} \cdot (\dot{\Gamma}_3 - \dot{\Gamma}_2)}{\dot{\Gamma}_2 \cdot \dot{\rho}_2 - \dot{\Gamma}_3 \cdot \dot{\rho}_3} \tag{6}$$

$$\dot{E}_{DF} = \dot{\rho}_1 - \dot{\Gamma}_1 \cdot (\dot{E}_{SF} \cdot \dot{\rho}_1 + \dot{\gamma}) \tag{7}$$

$$\dot{E}_{RF} = \dot{E}_{DF} \cdot \dot{E}_{SF} + \dot{\gamma} \tag{8}$$

$$\dot{\gamma} = \frac{(\dot{\rho}_2 - \dot{\rho}_1) \cdot (\dot{\Gamma}_2 \cdot \dot{\rho}_2 - \dot{\Gamma}_3 \cdot \dot{\rho}_3) + (\dot{\rho}_2 - \dot{\rho}_3) \cdot (\dot{\Gamma}_1 \cdot \dot{\rho}_1 - \dot{\Gamma}_2 \cdot \dot{\rho}_2)}{(\dot{\Gamma}_3 - \dot{\Gamma}_2) \cdot (\dot{\Gamma}_2 \cdot \dot{\rho}_2 - \dot{\Gamma}_1 \cdot \dot{\rho}_1) + (\dot{\Gamma}_1 - \dot{\Gamma}_2) \cdot (\dot{\Gamma}_3 \cdot \dot{\rho}_3 - \dot{\Gamma}_2 \cdot \dot{\rho}_2)} \tag{9}$$

The open-ended coaxial line shown in Figs. 1 and 2 can be represented as the equivalent circuit shown in Fig. 4, where C_f and $\varepsilon_{ri} \cdot C_0$ are defined as the fringing capacitance at the tip of the coaxial line and the sample insertion section at the coaxial tip, respectively. Here, $C_T = C_f + \varepsilon_{ri} \cdot C_0$ is satisfied. Accordingly, the input impedance $Z_{\Gamma i}$ for Ref. 2 (Port 2) is expressed by

$$\dot{Z}_{\Gamma i} = \frac{1}{j\omega \cdot C_T} = \frac{1}{j\omega \cdot (C_f + \dot{\varepsilon}_{ri} \cdot C_o)} \tag{10}$$

Thus, the reflection constant Γ_i for Ref. 2 (Port 2) can be calculated [15] by

$$\dot{\Gamma}_i = \frac{\dot{Z}_{\Gamma i} - Z_0}{\dot{Z}_{\Gamma i} + Z_0} = \frac{1 - j\omega C_0 \cdot \dot{\varepsilon}_{ri} \cdot Z_0 - j\omega C_f \cdot Z_0}{1 + j\omega C_0 \cdot \dot{\varepsilon}_{ri} \cdot Z_0 + j\omega C_f \cdot Z_0} \tag{11}$$

Here, Z_0 is the characteristic impedance of Port 1, defined as $Z_0 = 50\ \Omega$. Accordingly, the theoretical reflection coefficient Γ_i for Ref. 2 (Port 2) with the assumption of the reference material in the jig is then determined based on Eq. (11) by substituting the C_f and C_0 values of the equivalent circuit shown in Fig. 4. In the proposed S_{11} method, to improve accuracy in measurement of S_{11} against the conventional method [15], [17]–[19], C_f and C_0 in Eq. (10) are determined by substituting the input impedance calculated via the MM technique for the analysis model of Fig. 2 at each frequency into $Z_{\Gamma i}$ on the left side. Here, $Z_{\Gamma i}$ for open termination is determined by substituting $\varepsilon_{ri} = 1.0$ (air) into ε_{ri} in Eq. (10). Accordingly, E_{DF}, E_{RF} and E_{SF} (system errors in Eq. (5)) are determined based on Eqs. (6)–(9) from the theoretical value of the reflection constant Γ_i (where i = 1, 2 and 3) under the three termination conditions in Ref. 2 and the measured value of the reflection coefficient ρ_i in Ref. 1. Equation (5) is also transformed as below based on the relationship between the measured reflection coefficient ρ_{meas} from Ref. 1 and the reflection coefficient Γ_{corr} from Ref. 2 as calibrated from the theoretical value of the reflection coefficient Γ_i.

$$\dot{\Gamma}_{corr} = \frac{\dot{\rho}_{meas} - \dot{E}_{DF}}{\dot{E}_{SF} \cdot \dot{\rho}_{meas} + \dot{E}_{RF} - \dot{E}_{SF} \cdot \dot{E}_{DF}} \tag{12}$$

From the above relationship, the calibrated reflection coefficient Γ_{corr} for Ref. 2 (Port 2) is obtained by substituting the measured ρ_{meas} value for Ref. 1 (Port 1) and the E_{DF}, E_{RF} and E_{SF} values determined from the three termination conditions into Eq. (12).

In this method, the S_{11} value of the jig is calibrated with three reference materials (including air) using Eq. (12). The procedure for S_{11} calibration with the jig based on substitution of the electrostatic capacitance value determined from the equivalent circuit is outlined below.

1. The electrostatic capacitance C_f of the coaxial part is determined by comparing the input impedance calculated via EM analysis to the analytical model assuming the complex permittivity of the sample as $\varepsilon_{ri} = 1.0$ (air).
2. The electrostatic capacitance C_0 value for the circular cavity section at each frequency is determined from the above C_f value, the complex permittivity for each reference material inserted and the reflection constant calculated via EM analysis.
3. The theoretical value of the reflection coefficient Γ_i for Ref. 2 (Port 2) with assumed insertion of the three reference materials is determined based on Eq. (11) by substituting the complex permittivity for each material and the C_f and C_0 values.
4. The theoretical value of the reflection constant Γ_i for Ref. 2 as determined above and the measured reflection constant ρ_i for Ref. 1 are substituted into Eqs. (6)–(9).
5. E_{DF}, E_{RF} and E_{SF} in the measurement system are determined based on Eqs. (6)–(9).
6. The measured S_{11} value for Ref. 2 after calibration is determined from Eq. (12) by substituting the above E_{DF}, E_{RF}, E_{SF} values and the measured reflection constant ρ_{meas} for Ref. 1

The procedure for determination of actual electrostatic capacitance is outlined in the next chapter.

3. Quantification of Electrostatic Capacitance at the Measurement Jig Tip

The capacitance of the coaxial tip is first quantified for calibration of the coaxial line S_{11} value using a VNA in the above procedure. To this end, the input impedance assuming insertion of the three reference materials with correspondence to the analytical model of Fig. 2 is first calculated based on EM analysis via the MM technique. Here, pure water, methanol and air were used as the three standard materials as necessary for S_{11} calibration. Next, for calculation of the reflection constant based on equivalent analysis, the calculated values of input impedance for each insertion condition for Ref. 2 from the MM technique were

Table 1 Determination of C_f with Eq. (14) based on $\varepsilon_{ri} = 1.0 - j\,0.0$

Frequency [GHz]	$Z_{\Gamma i}$ determined using the MM technique [Ω]	C_f based on Eq. (14) [pF]
0.50	0.00 –j 9734.6	0.021978
1.5	0.00 –j 3244.0	0.021984
3.0	0.00 –j 1620.5	0.022040

substituted into the left side of Eq. (10). The electrostatic capacitance C_f and the C_0 value of the equivalent circuit shown in Fig. 4 were then determined based on the procedure outlined below.

Two capacitances are connected in parallel at the front of the transmission line expressed by the equivalent circuit as shown in Fig. 4 with correspondence to the analytical model of Fig. 2. Here, C_f and C_0 are the electrostatic (fringing) capacitances of the coaxial line and the sample insertion section. It is also assumed that $C_f \equiv \varepsilon_{rA} \cdot C_0$ is satisfied for $\varepsilon_{ri} = 1.0 - j\,0.0$. The total capacitance of C_f and C_0 is then calculated as $C_T = C_f + \varepsilon_{ri} \cdot C_0$. Based on the results, the total capacitance at the coaxial tip is defined as $C_T \equiv C_f + C_f/\varepsilon_{rA}$. Input impedance for Ref. 2 is expressed as $Z_{\Gamma i} = R_{\Gamma i} + jX_{\Gamma i}$ using Eq. (10), and $R_{\Gamma i} = 0\Omega$ is satisfied in the case of $\varepsilon_{ri} = 1.0 - j\,0.0$. Accordingly, $Z_{\Gamma i}$ is simplified to a pure imaginary value, and input impedance can be expressed as

$$Z_{\Gamma i} = jX_{\Gamma i} = \frac{1}{j\omega \cdot C_T} \equiv \frac{\varepsilon_{rA}}{j\omega \cdot C_f \cdot (\varepsilon_{rA} + 1)} \tag{13}$$

C_f is thus expressed as follows by manipulating Eq. (13) with focus on C_f:

$$C_f \equiv \frac{\varepsilon_{rA}}{j^2 \cdot \omega \cdot (1+\varepsilon_{rA}) \cdot X_{\Gamma i}} = -\frac{\varepsilon_{rA}}{\omega \cdot (1+\varepsilon_{rA}) \cdot X_{\Gamma i}} \tag{14}$$

The electrostatic capacitance C_f of the coaxial line section can be calculated via the above procedure. Meanwhile, $R_{\Gamma i} = 0$ is also determined from input impedance ($Z_{\Gamma i} = R_{\Gamma i} + jX_{\Gamma i}$) based on EM analysis via the MM technique, as the real part of input impedance is 0 Ω with an open coaxial tip. As a result, $Z_{\Gamma i} = jX_{\Gamma i}$ is satisfied. C_f was then determined by substituting the value of $Z_{\Gamma i}$ calculated using the MM technique and ε_{rA} into Eq. (14). The frequencies for calculation were set as 0.50, 1.5 and 3.0 GHz from past research results. The $Z_{\Gamma i}$ [Ω] values for input impedance calculated using the MM technique with 2a = 4.10 mm, 2b = 1.30 mm, d = 5.00 mm and $\varepsilon_{rA} = 2.05$ (Fig. 1) are shown in Table 1. The electrostatic capacitance C_f of the coaxial line section for each frequency was also calculated as shown in Table 1 by substituting the above $Z_{\Gamma i} = jX_{\Gamma i}$ into Eq. (14).

Next, the electrostatic capacitance C_0 at the circular cavity (sample insertion) section was determined from the fringing capacitance C_f value for the coaxial line section as determined from the above procedure. For this purpose, the following equation is determined by manipulating Eq. (11) related to the theoretical value of the reflection coefficient Γ_i for Ref. 2, the electrostatic capacitances C_f and C_0, the line impedance Z_0 and the dielectric constant of the sample ε_{ri} with focus on C_0:

Table 2 C_0 values based on substitution of $Z_{\Gamma i}$ calculated using the MM Technique assuming the insertion of pure water in Eq. (15)

Freq. [GHz]	Permittivity determined using the Debye-relaxation equation ε_{r1}	Input impedance determined using the MM method $Z_{\Gamma 1}$ [Ω]	Capacitance determined using Eq. (15) C_0 [pF]
0.50	78.50 –j 1.912	3.4686 –j 142.79	0.028101
1.5	78.11 –j 5.705	3.4694 –j 46.785	0.028599
3.0	76.80 –j 11.21	3.4859 –j 21.943	0.030481

Table 3 C_0 values based on substitution of $Z_{\Gamma i}$ calculated using the MM technique assuming the insertion of methanol in Eq. (15)

Freq. [GHz]	Permittivity determined using Debye-relaxation equation ε_{r2}	Input impedance determined using MM technique $Z_{\Gamma 2}$ [Ω]	Capacitance determined using Eq. (15) C_0[pF]
0.50	36.48 –j 4.814	39.392 –j 301.07	0.027901
1.5	31.66 –j 12.27	39.373 –j 101.56	0.028093
3.0	22.51 –j 16.27	38.892 –j 52.753	0.028502

$$C_0 = \frac{1}{\dot{\varepsilon}_{ri}} \cdot \left[\frac{1}{j\omega \cdot Z_0} \left(\frac{1 - \dot{\Gamma}_i}{1 + \dot{\Gamma}_i} \right) - C_f \right] \tag{15}$$

In the proposed method, S_{11} is calibrated by substituting Γ_i (the theoretical value of the reflection coefficient for Ref. 2 with the assumption of each sample in the jig analysis model) and ρ_i (the actual measurement value of the reflection coefficient for Ref. 1) into Eqs. (5) to (9). Here, the theoretical value of the reflection coefficient for Ref. 2 is calculated using Eq. (11) corresponding to the equivalent circuit shown in Fig. 4 to shorten the computation time. The electrostatic capacitance C_0 of the sample insertion part necessary for calculation of the reflection coefficient based on the above equivalent circuit is also calculated using Eq. (15). In [15], the VNA-measured value was substituted as the reflection coefficient Γ_i in Eq. (15). Here, the value calculated (exact solution) using the MM technique is substituted into Γ_i to improve the accuracy of the S_{11} calibration value. The theoretical value (i.e., the calculated complex number) determined using the Debye dispersion equation [11], [20], [21] is substituted as the complex permittivity part ε_{ri} of Eq. (15) for each sample. Accordingly, capacitance C_0 is also calculated as a complex number with its imaginary part uniquely corresponding to the dielectric loss tangent of the sample. Here, pure water (ε_{r1}), methanol (ε_{r2}) and air ($\varepsilon_{r3} = 1.0$) were the three reference materials. In this study, the complex permittivity of the reference material used to determine C_0 was calculated from the theoretical value using the Debye dispersion equation [11], [20], [21]. Moreover, various investigations were carried out with complex permittivity calculated using the Debye dispersion formula corrected from on past evaluation conducted by the author. Specifically, based on Eq. (27) in Ref. [21], the values of $\varepsilon_0 = 37.2$, $\varepsilon_{inf} = 4.49$ and $\tau = 4.78 \cdot 10^{-11}$ were used to calculate complex permittivity for methanol at a liquid temperature of 25.0°C based on previous measurements made by the author [14]. The results of calculation to determine input impedance $Z_{\Gamma 1}$ using the MM technique with a condition of complex permittivity ε_{ri} using the Debye-dispersion

equation [21] at a liquid temperature of 25.0°C for each frequency are shown in Tables 2 and 3. Accordingly, electrostatic capacitance C_0 at the sample insertion section was calculated by substituting the values of C_f, Z_0, ε_{ri} and $Z_{\Gamma i}$ (Γ_i) into Eq. (15). The results with the insertion of pure water and methanol are shown in Tables 2 and 3.

The electrostatic capacitance C_0 of the sample insertion part was also calculated for air ($\varepsilon_{r3} = 1.0$). The total value at the tip of the coaxial line was determined using $C_T \equiv C_f + \varepsilon_{r3} \cdot C_0$, and $C_f \equiv \varepsilon_{rA} \cdot C_0$ was assumed for $\varepsilon_{r3} = 1.0$. Thus, $C_0 \equiv C_f/\varepsilon_{rA}$ was set. The value for the sample insertion section can thus be immediately determined by substituting the values of C_f and ε_{rA} into above equation, and the results of calculation to determine C_0 for each frequency with sample insertion of air are shown in Table 4.

The input impedance $Z_{\Gamma i}$ (where i = 1, 2 and 3) for Ref. 2 was also calculated using C_f and C_0 values determined via the above procedure. Here, pure water, methanol and air were assumed as reference materials for jig insertion. The input impedance $Z_{\Gamma i}$ for Ref. 2 was calculated by substituting the values of Table 2–4 for complex permittivity and the values of C_f and C_0 into Eq. (11). These values were compared with those from the MM technique (see Tables 5 to 7). The values calculated from Eq. (11) correspond exactly to those of the MM technique, indicating that input impedance on the front surface of the sample can be accurately calculated by substituting C_f and C_0 for the equivalent circuit as determined from Eqs. (14) and (15) into Eq. (11) with a coaxial-feed type cut-off circular waveguide as with the measuring jig.

Table 4 C_0 values based on the assumption of an open termination condition ($\varepsilon_{r3} = 1.0$)

Frequency [GHz]	Complex permittivity ε_{r3}	C_0 [pF]
0.50	1.00 –j 0.00	0.0107210
1.5	1.00 –j 0.00	0.0107239
3.0	1.00 –j 0.00	0.0107338

Table 5 Input impedance with the complex permittivity values in Table 2, C_f and C_0 substituted into Eq. (11) (pure water)

Freq. / $Z_{\Gamma 1}$	0.50 GHz	1.5 GHz	3.0 GHz
$Z_{\Gamma 1}$ determined using Eq. (11) [Ω]	3.4686 –j 142.79	3.4694 –j 46.785	3.4859 –j 21.943
$Z_{\Gamma 1}$ determined using MM Technique [Ω]	3.4686 –j 142.79	3.4694 –j 46.785	3.4859 –j 21.943
Difference [%]	0.00 (Real) 0.00 (Imag.)	0.00 (Real) 0.00 (Imag.)	0.00 (Real) 0.00 (Imag.)

Table 6 Input impedance with the complex permittivity values in Table 3, C_f and C_0 substituted into Eq. (11) (methanol)

Freq. / $Z_{\Gamma 2}$	0.50 GHz	1.5 GHz	3.0 GHz
$Z_{\Gamma 2}$ determined using Eq. (11) [Ω]	39.392 –j 301.07	39.273 –j 101.56	38.892 –j 52.753
$Z_{\Gamma 2}$ determined using MM Technique [Ω]	39.392 –j 301.07	39.273 –j 101.56	38.892 –j 52.753
Difference [%]	0.00 (Real) 0.00 (Imag.)	0.00 (Real) 0.00 (Imag.)	0.00 (Real) 0.00 (Imag.)

Table 7 Input impedance with the complex permittivity values in Table 4, C_f and C_0 substituted into Eq. (11) (air)

Freq. / $Z_{\Gamma 3}$	0.50 GHz	1.5 GHz	3.0 GHz
$Z_{\Gamma 3}$ determined using Eq. (11) [Ω]	$-2.1854 \cdot 10^{-2}$ –j 9734.6	$+4.3980 \cdot 10^{-4}$ –j 3244.0	$-1.0850 \cdot 10^{-3}$ –j 1620.5
$Z_{\Gamma 3}$ determined using MM Technique [Ω]	0.00 –j 9734.6	0.00 –j 3244.0	0.00 –j 1620.5
Difference [%]	0.00 (Imag.)	0.00 (Imag.)	0.00 (Imag.)

4. Verification of S_{11} Calibration Accuracy

The validity of reflection coefficient Γ_{corr} calibration based on Eqs. (6)–(15) via the procedure described in Sects. 2 and 3 was verified at frequencies of 0.50, 1.5 and 3.0 GHz with pure water, methanol and air as reference materials at a liquid temperature of 25.0°C. Here, dielectric constant setting is required in calculation of the theoretical reflection coefficient Γ_i for the reference material. The calculated value from the Debye dispersion equation [20] was thus set for pure water, the equation corrected from the value measured by the author [14] was set for methanol, and the theoretical value (1.0 – j0.0) was set for air (open) as shown in Tables 2–4. The dimensions and electrical constants of the analytical model as shown in Figs. 1 and 2 were set as 2a = 4.10 mm, 2b = 1.30 mm, d = 5.00 mm and $\varepsilon_{ra} = 2.05$. The theoretical reflection constant Γ_i based on the equivalent circuit for Ref. 2 with the insertion of each reference material and setting of the above dielectric constant ε_{ri} was used based on extraction from the values calculated using Eq. (11) (Tables 5 to 7). Meanwhile, the S_{11} value at the tip of the coaxial cable connected to the VNA was calibrated using a general SOL (short, open and loaded) calibration kit, and the jig shown in Fig. 1 was connected to the tip of the cable for actual S_{11} measurement. The reflection constant on the SOL calibration plane (Ref. 1) for substitution into ρ_i (where i = 1, 2 and 3) in Eqs. (6)–(9) (as necessary for S_{11} calibration at the front of the sample (Ref. 2) using the measurement system) was measured in the frequency range of 0.50 to 3.0 GHz with pure water, methanol and open termination conditions. Results of input impedance measurement at 0.50, 1.5 and 3.0 GHz are shown in Table 8.

Table 8 Input impedance measurement values with reference material insertion (25.0°C) for the SOL calibration plane (Ref. 1) in S_{11} calibration

Condition	Frequency [GHz]		
	0.50	1.5	3.0
Pure water Z_{meas1}	2.0754 –j 106.66	2.2970 –j 22.765	3.2045 –j 13.189
Methanol Z_{meas2}	14.176 –j 166.50	14.647 –j 47.621	16.617 –j 9.6530
Open Z_{meas3}	1.0359 –j 416.01	0.44183 –j 133.31	0.23407 –j 56.695

Table 9 Input impedance measurement values for the SOL calibration plane (Ref. 1) for S_{11} calculation at the front of the sample (Ref. 2)

Condition	Frequency [GHz]		
	0.50	1.5	3.0
Pure water Z_{meas1}	2.0416 –j 106.54	2.2971 –j 22.722	3.2138 –j 13.231
Methanol Z_{meas2}	14.045 –j 165.43	14.575 –j 47.208	16.581 –j 9.3088
Open Z_{meas3}	0.73658 –j 416.14	0.45004 –j 133.32	0.26302 –j 56.660
Ethanol Z_{meas4}	36.793 –j 216.61	26.491 –j 79.654	15.546 –j 35.803

Input impedance on the SOL calibration plane (Ref. 1) was also measured for the tip of the jig with open, pure water, methanol and ethanol as unknown materials for substitution of the value as the reflection constant (ρ_{meas}) in Eq. (12) to calibrate S_{11} at the front surface of the sample (Ref. 2) under various conditions after jig mounting (Table 9), and S_{11} calibration for the sample front of the jig was performed using these values. Here, the relationship between complex permittivity estimated using the proposed method and the accuracy (uncertainty) of input impedance measurement values was examined. As an example, the variation of measured input impedance with respect to Z_{in} = 2.0416 – j 106.54 at a frequency of 0.50 GHz with pure water inserted as shown in Table 9 was first considered. For these sample insertion conditions, variations of 0.05 for the real part and 0.2 for the imaginary part are assumed due to the uncertainty (accuracy) of the VNA used in measurement. The variation in the estimated value of complex permittivity (78.50 – j 1.922) associated with the variation in the measured value of Z_{in} was calculated as an inverse problem via the MM technique. The results showed changes of 0.187 in the real part and 0.054 in the imaginary part. The real part of complex permittivity also changed by 0.098 and the imaginary part by 0.002 with the variation of the outer-conductor's inner diameter (2a) of 0.05 mm in Ref. [4]. Accordingly, complex permittivity in each table was unified to four significant digits for both the real and imaginary parts. Input impedance was also unified to five significant digits for both parts.

S_{11} at the front surface of the sample (Ref. 2) with the jig for permittivity measurement attached to the tip of the coaxial cable of the measurement system was calibrated using the input impedance value measured on the SOL calibration plane (Ref. 1) as described above. Here, the theoretical input impedance in Ref. 2 converted to the reflection coefficient Γ_i with pure water, methanol and open conditions calculated using Eq. (11) (Tables 5 to 7) was first substituted into Eqs. (6) to (9). Input impedance measured on the SOL calibration plane (Ref. 1) converted to the reflection coefficient ρ_i with pure water, methanol and open conditions on the sample front (as required for S_{11} calibration of the jig) (Table 8) was also substituted into the ρ_i part of Eqs. (6) to (9). E_{DF}, E_{SF} and E_{RF}, representing the error term of the measurement system and the auxiliary function γ of the above values, are then calculated (as required for S_{11} calibration at the front surface of the sample in the jig). Moreover, input impedance measured on the SOL calibration plane (Ref. 1) converted to the reflection coefficient ρ_{meas} on the sample front (as required for S_{11} calibration of the jig) with pure water, methanol and ethanol inserted as unknown materials (Table 9) was substituted into the ρ_{meas} part of Eq. (12). The reflection coefficient at the front of the sample after calibration (Ref. 2) under each termination condition was thus calibrated as Γ_{corr} using Eq. (12) at each frequency from the above procedure. The measured reflection constants Γ_{corr} after calibration based on Eqs. (5)–(12) at frequencies of 0.50, 1.5 and 3.0 GHz and a liquid temperature of 25.0°C were then verified. The input impedance measurement results for various liquid types after calibration with the three materials are shown in Table 10, which also indicates measured values after SOM calibration (short, open and reference material (pure-water)) conditions. The error of the results based on Eq. (12) was within 0.02% with pure water as the unknown material, 2.0% with methanol and 1.1% with air (open). Comparison of measured input impedance after calibration with the three reference mate-

Table 10 Input impedance at the front of the sample (Ref. 2) after calibration with three termination conditions (25.0°C)

(a) Open

Condition	Frequency [GHz]		
	0.50	1.5	3.0
Calibration with three reference materials	–171.83 –j 9804.3	4.4254 –j 3249.1	14.364 –j 1604.1
SOM calibration [14]	–171.71 –j 9804.1	4.4111 –j 3249.1	14.209 –j 1603.8
Inter-value difference [%]	–0.070 +0.714	–0.323 +0.158	–1.084 –1.032

(b) Pure water

Condition	Frequency [GHz]		
	0.50	1.5	3.0
Calibration with three reference materials	3.4086 –j 142.57	3.4665 –j 46.718	3.4904 –j 21.898
SOM calibration [14]	3.4083 –j 142.57	3.4667 –j 46.718	3.4911 –j 21.898
Inter-value difference [%]	–0.008 0.000	+0.006 –0.001	+0.020 +0.002

(c) Methanol

Condition	Frequency [GHz]		
	0.50	1.5	3.0
Calibration with three reference materials	39.392 –j 301.07	39.273 –j 101.56	38.892 –j 52.753
SOM calibration [14]	39.554 –j 301.26	39.359 –j 102.11	38.131 –j 53.049
Inter-value difference [%]	+0.412 +0.063	+0.218 +0.534	–1.955 +0.561

(d) Ethanol

Condition	Frequency [GHz]		
	0.50	1.5	3.0
Calibration with three reference materials	137.55 –j 401.73	129.74 –j 159.26	112.17 –j 110.41
SOM calibration [14]	137.91 –j 401.99	130.14 –j 161.33	109.97 –j 111.23
Inter-value difference [%]	+0.263 +0.065	+0.309 +1.298	–1.965 +0.742

rials and insertion of methanol with the results obtained after SOM calibration indicated a slight difference for the real part at 3.0 GHz. This may be attributed to variations observed in repeated measurement of S_{11}. Errors in input impedance measurement after calibration based on Eq. (12) were also within 2.0% with ethanol as the unknown material, which differed from outcomes observed with the reference materials. These details indicate that input impedance can be calibrated at a calculation accuracy within 2% even with various liquids assumed as unknown materials using a VNA with the proposed method. The results showed calibration values close to those observed from SOM conditions with the three reference materials. In addition, realization of a short condition in a coaxial feed-type cut-off circular waveguide is challenging. Specifically, the measured value of S_{11} after calibration is affected by the unstable nature of electrical contact with the coaxial tip with the short element in the jig with S_{11} calibration based on SOM. Here, instability factors relating to short termination with placement in the cut-off circular waveguide are eliminated by S_{11} calibration with three reference materials and no short termination. Such calibration is considered to enable measurement of permittivity with higher accuracy than SOM-based calibration.

5. Dielectric Measurement with Various Liquids

The dielectric constants of various liquids were estimated as an inverse problem based on comparison of 1. the S_{11} value measured with an unknown material in the jig, and 2. that calculated using the MM technique with a similar analytical model [4] from input impedance measured with liquids in the jig after S_{11} calibration at the front of the sample using three termination conditions. The effectiveness of the proposed S_{11} calibration method was verified by comparing the above estimated values with otherwise obtained outcomes after SOM calibration [14] and the theoretical value from the Debye relaxation equation [11], [14], [20], [21]. The results of dielectric constant estimation for pure water after calibration are shown in Table 11 (a). Values estimated as an inverse problem via the MM technique after calibration with the three reference materials were also compared with theoretical values obtained using the Debye dispersion formula, with results showing an exact match for all frequencies. The results from estimation as an inverse problem via the MM technique after SOM calibration were also compared with those calculated using the Debye dispersion formula, with differences of no more than 1.5% for all frequencies. This is attributed to the fact that the calibration procedure for S_{11} based on the three reference materials and SOM both involved the complex permittivity of pure water calculated using the Debye dispersion formula. The estimated dielectric constants of methanol (Table 11 (b)) also indicate an exact match between values estimated after calibration with the three reference materials and calculated using the Debye dispersion equation. This is attributed to the fact that calibration for S_{11} based on these materials involved the complex permittivity of methanol calculated using the Debye dispersion formula. Values estimated as an inverse problem via the MM technique after calibration with the three reference materials were also compared with values estimated as an inverse problem via the MM technique after

Table 11 Results of complex permittivity estimation for various liquids

(a) Pure water (25.0°C)

Condition	Frequency [GHz]		
	0.50	1.5	3.0
Inverse problem with MM technique after calibration with three reference materials	78.62 –j 1.884	78.22 –j 5.716	76.94 –j 11.26
Inverse problem with MM technique after SOM calibration [14]	78.62 –j 1.884	78.22 –j 5.716	76.94 –j 11.26
Debye dispersion formula [20]	78.50 –j 1.912	78.11 –j 5.705	76.80 –j 11.21
Difference between calibration with three reference materials and SOM	0.0 0.0	0.0 0.0	0.0 0.0
Difference between calibration with three reference materials and Debye dispersion formula [%]	+0.150 –1.444	+0.141 +0.202	+0.175 +0.512
Difference between SOM calibration and Debye dispersion formula [%]	+0.150 –1.444	+0.141 +0.202	+0.175 +0.512

(b) Methanol (25.0°C)

Condition	Frequency [GHz]		
	0.50	1.5	3.0
Inverse problem with MM technique after calibration with three reference materials	36.48 –j 4.814	31.66 –j 12.27	22.51 –j 16.27
Inverse problem with MM technique after SOM calibration [14]	36.45 –j 4.827	31.52 –j 12.18	22.77 –j 16.05
Debye dispersion formula [14], [21]	36.48 –j 4.814	31.66 –j 12.27	22.51 –j 16.27
Difference between calibration with three reference materials and SOM	+0.081 –0.273	+0.454 +0.762	–1.135 +1.400
Difference between calibration with three reference materials and Debye dispersion formula [%]	0.0 +0.01	0.00 –0.01	0.00 +0.02
Difference between MM technique after SOM calibration and Debye dispersion formula [%]	–0.076 +0.274	–0.452 –0.756	+1.148 –1.383

(c) Ethanol (25.0°C)

Condition	Frequency [GHz]		
	0.50	1.5	3.0
Inverse problem with MM technique after calibration with three reference materials	24.78 –j 8.598	13.83 –j 11.48	8.039 –j 8.355
Inverse problem with MM technique after SOM calibration [14]	24.76 –j 8.606	13.76 –j 11.38	8.204 –j 8.292
Coaxial probe method [12]	24.60 –j 8.163	13.07 –j 10.42	8.181 –j 6.953
Difference between calibration with three reference materials and SOM	+0.107 –0.093	+0.504 +0.889	–2.010 +0.765
Difference between MM technique after calibration with three reference materials and Coaxial probe method [%]	+0.730 +5.320	+5.821 +10.189	–1.726 +20.173
Difference between MM technique after SOM calibration and Coaxial probe method [%]	+0.622 +5.418	+5.290 +9.218	+0.290 +19.261

SOM calibration and theoretical values obtained using the Debye dispersion formula. The values showed differences of no more than 1.4% at all frequencies. Estimation results for the dielectric constant of ethanol are shown in Table 11 (c). In this case, the complex permittivity of ethanol was also estimated via the coaxial-probe method [12], [13]. Values estimated as an inverse problem via the MM technique after calibration with the three reference materials were compared with those estimated as an inverse problem via the MM technique after SOM calibration. The values showed differences of no more than 2.01% for all frequencies. However, differences among values were found to increase with frequency. Next, values estimated as an inverse problem via the MM technique after calibration with the three reference materials and SOM calibration were compared with those estimated as an inverse problem via the coaxial probe method [12], [13]. The values showed differences of no more than 5.83% for the real part for all frequencies. However, differences among values for the imaginary part were found to increase with frequency. However, the close agreement between estimation values after calibration with the three reference materials and those after SOM calibration indicates the validity of the proposed S_{11} calibration and permittivity estimation.

6. Conclusion

This study involved verification of an S_{11} calibration method for jigs to improve measurement accuracy in the estimation of dielectric constants from measured S_{11} values with various liquids in an open-ended cut-off waveguide. Specifically, termination conditions with three reference materials were used for calibration at the front surface of the material for the jig with the material inserted for estimation of the complex permittivity of various liquids. Moreover, the electrostatic capacitance for the analytical model unique to the jig was quantified by substituting the reflection constant (calculated using the mode-matching (MM) technique) into the equivalent circuit, assuming the sample liquid in the jig. With pure water, methanol and air as the reference materials, S_{11} was calibrated at the front of the sample in the jig within the frequency band of 0.50–3.0 GHz, and S_{11} was measured at the front of the sample with various liquids in the jig after calibration. The validity of the calibrated S_{11} values obtained with the proposed method was verified via comparison with the S_{11} value measured after SOM calibration conditions. S_{11} at the front surface of the sample was measured with various liquids in the jig after calibration with three reference materials, and the dielectric constants of various liquids were estimated from the above S_{11} based on an inverse problem approach involving comparison with the S_{11} value calculated using EM analysis via the MM technique. The results were compared with the permittivity values estimated as an inverse problem after SOM calibration conditions and similar, with results showing favorable agreement of values determined with each method. Future work will involve evaluation of actual liquids and their temperature dependence along with extension of the method to examination of liquids in the millimeter range. Round-robin testing at different institutions is also necessary in association with standardization of this method.

Acknowledgements

This work was partly supported by a Grant-in-Aid for Scientific Research (No. 20K04522; Establishment of a Broadband Dielectric Measurement Method for Liquids in Temperature-Change Environments for Synthesis of Functional Materials) from the Japan Society for the Promotion of Science (JSPS).

References

[1] A. Hirata, S. Kodera, J. Wang, and O. Fujiwara, "Dominant factors for influencing whole-body average SAR due to far-field exposure in whole-body resonance frequency and GHz regions," Bioelectromagnetics, vol.28, pp.484–487, 2007.
[2] M.A. Stuchly and S.S. Stuchly, "Coaxial Line Reflection Methods for Measuring Dielectric Properties of Biological Substances at Radio and Microwave Frequencies – A Review," IEEE Trans. Instrum. Meas., vol.IM-29, no.3, pp.176–183, Oct. 1980.
[3] O. Göttmann, U. Kaatze, and P. Petong, "Coaxial to circular waveguide transition as high-precision easy-to-handle measuring cell for the broad band dielectric spectrometry of liquids," Measurement Science and Technology, vol.7, no.4, pp.525–534, April 1996.
[4] K. Shibata, "Measurement of Complex Permittivity for Liquid Materials Using the Open-ended Cut-off Waveguide Reflection Method," IEICE Trans. Electron., vol.E93-C, no.11, pp.1621–1629, Nov. 2010.
[5] K. Shibata, "Broadband measurement of complex permittivity for liquids using the open-ended cut-off circular waveguide reflection method," 35th PIERS Proceedings, Guangzhou, China, pp.2,079–2,084, Aug. 2014.
[6] K. Shibata and M. Kobayashi, "Broadband Measurement of Complex Permittivity for Liquids via the Open-ended Cut-off Waveguide Reflection Method Using a Large-bore Connector," Proc. 45th European Microwave Conf., EuMC 2015, Paris, France, pp.979–982, Sept. 2015.
[7] K. Shibata and M. Kobayashi, "Simplification of Liquid Dielectric Property Evaluation Based on Comparison with Reference Materials and Electromagnetic Analysis Using the Cut-off Waveguide Reflection Method," IEICE Trans. Electron., vol.E100-C, no.10, pp.908–917, Oct. 2017.
[8] K. Shibata, "Method for Dielectric Measurement in Liquids Using an Estimation Equation without Short Termination," Proc. 22nd International Microwave and Radar Conference, MIKON 2018, Poznan, Poland, pp.751–754, May 2018.
[9] K. Shibata, "Dielectric Measurement in Liquids Using an Estimation Equation without Short Termination via the Cut-Off Circular Waveguide Reflection Method," IEICE Trans. Electron., vol.E101-C, no.8, pp.627–636, Aug. 2018.
[10] K. Shibata, "Improvement in liquid permittivity measurement using the cut-off waveguide reflection method," Proc. 1st European Microwave Conference in Central Europe, EuMCE 2019, Prague, Czech Republic, May 2019.
[11] A.P. Gregory and R.N. Clarke, "Tables of the complex permittivity of dielectric reference liquids at frequencies up to 5 GHz," NPL Report Mat. 23, pp.1–87, Jan. 2012.
[12] K. Shibata and M. Kobayashi, "Difference Between the Method of Moments and the Finite Element Method for Estimation of Complex Permittivity in Liquids Using a Coaxial Probe," Proc. EMC Europe

2019, pp.100–105, Barcelona, Spain, Sept. 2019.
[13] K. Shibata and M. Kobayashi, "Dielectric Property Measurement Errors Based on Application of an Estimation Equation Using the Coaxial Probe Method," Proc. 7th IEEE MTT-S International Microwave & RF Conference, IMaRC 2019, pp.1–5, Mumbai, India, Dec. 2019.
[14] K. Shibata, "S11 Calibration Method for a Coaxial-loaded Cut-off Circular Waveguide using SOM Termination," Proc. 2020 IEEE Sensors Applications Symposium, IEEE SAS 2020, Kuala Lumpur, Malaysia, March 2020.
[15] A. Kraszewski, M.A. Stuchly, and S.S. Stuchly, "ANA Calibration Method for Measurement of Dielectric Properties," IEEE Trans. Instrum. Meas., vol.IM-32, no.2, pp.385–387, June 1983.
[16] "HP 85070B Dielectric Probe Kit, User's Manual," Hewlett-Packard, HP part number 85070-90009, April 1993.
[17] S. Rehnmark, "On the Calibration Process of Automatic Network Analyzer Systems," IEEE Trans. Microw. Theory Techn., vol.MTT-22, no.4, pp 457–458, April 1974.
[18] D. Rytting, "Network Analyzer Error Models and Calibration Methods," Agilent Technology Application Note.
[19] "HP 8753D Network Analyzer, User's Guide," Hewlett-Packard, HP part number 08753-90257, Oct. 1997.
[20] U. Kaatze, "Complex Permittivity of Water as a Function of Frequency and Temperature," J. Chem. Eng. Data, 1989, vol.34, no.4, pp.371–374, Oct. 1989.
[21] T.J. Ikyumbur, M.Y. Onimisi, S.G. Abdu, E.C. Hemba, and Z.J. Kirji, "Optimization in the Computation of Dielectric Constants of Methanol Using the Debye Relaxation Method," British Journal of Applied Science & Technology, vol.19, no.1, pp.1–10, Feb. 2017.

Kouji Shibata was born in Shimada City, Shizuoka Prefecture, Japan, in 1970. After graduating from the Engineering Department at the Kanazawa Institute of Technology in Ishikawa, Japan, in 1993, he took up employment with SPC Electronics (Shimada Physical & Chemical Industrial) Co., Ltd. in Chofu, Japan. His roles there included designing and developing passive circuits such as filters, couplers, diplexers and antennas in the microwave/millimeter band. In 2001 and 2004, respectively, he completed the Master's and Doctoral Programs of Aoyama Gakuin University Graduate School in Tokyo, Japan, and holds Doctor of Engineering status. In 2004 he took up a position as a lecturer at Hachinohe Institute of Technology in Japan and became an associate professor in 2015. He is currently engaged in research on electrical constant measurement for passive components in the high-frequency band and the development of a small sensor information mobile Internet communication system using an ARM microcomputers running on Linux.